Simultaneous FTIR Emission Spectroscopy and Chemiluminescence of Oxidizing Polypropylene: Evidence for Alternate Chemiluminescence Mechanisms

Idriss Blakey and Graeme A. George*

Centre for Instrumental and Developmental Chemistry, School of Physical Sciences, Queensland University of Technology, Brisbane, Queensland, Australia

Received July 11, 2000; Revised Manuscript Received December 18, 2000

ABSTRACT: The thermal oxidation of polypropylene was probed, in situ, by a novel technique that simultaneously monitors chemically induced light emission (chemiluminescence) and changes in FTIR emission spectra of an oxidizing sample. The results obtained from this technique demonstrated that the chemiluminescence intensity (I_{CL}) was proportional to the accumulation of carbonyl species formed during oxidation, rather than the rate of oxidation, which is predicted from application of the steady-state approximation to classical chemiluminescence mechanisms associated with auto-oxidation. Two possible mechanisms were proposed to account for the results obtained. The first mechanism involved energy transfer from a triplet carbonyl, formed via a classical mechanism, to a more efficient emitter formed during oxidation. The second possible mechanism involved reaction of a peroxidic compound with an oxidation product.

Introduction

Free radical oxidation of polymers[1−3] and organic compounds[4−7] (see Scheme 1) leads to emission of low levels of visible light, which is commonly termed chemiluminescence (CL). CL analysis can be used to probe oxidation reactions in real time and with high sensitivity.[8] However, there has been reluctance to adopt this technique for routine analysis of polymer degradation. Largely, this reluctance has been perceived to be due to uncertainties regarding the chemiluminescence mechanism, and consequently interpretation of data obtained from this technique. Factors such as low quantum efficiencies hinder studies of the mechanism because the CL process may be obscured by parallel nonchemiluminescent reactions, which constitute the bulk of auto-oxidation reactions.

Information on the mechanism can be gained from the wavelength range of the light emitted. During oxidation of polypropylene (PP), the majority of light emitted is from the 360−460 nm region,[9−11] which is consistent with emission during the relaxation of triplet carbonyls to the ground state. However, identification of the light emitting species cannot be determined with certainty because emission spectra lack uniquely characteristic bands. Other evidence such as the effect of triplet sensitizers on light intensity[12,13] and quenching of CL by oxygen,[4,14] indicate that relaxation of a triplet excited state is a source of light emission. The total luminous intensity (TLI) emitted when an oxidized polymer is heated in an inert atmosphere has been shown to be proportional to the concentration of titratable peroxides during the early stages of oxidation.[15,16] This evidence indicates that the mechanism involves peroxidic groups or radicals that are produced during peroxide decomposition.[17]

Reactions that have been proposed to generate triplet carbonyls are termination of peroxy radicals [6,18,19] via the Russell mechanism[8,15,20,21] and decomposition of hydroperoxides.[22−24]

Scheme 1

Basic Autoxidation Scheme

Chain Initiation

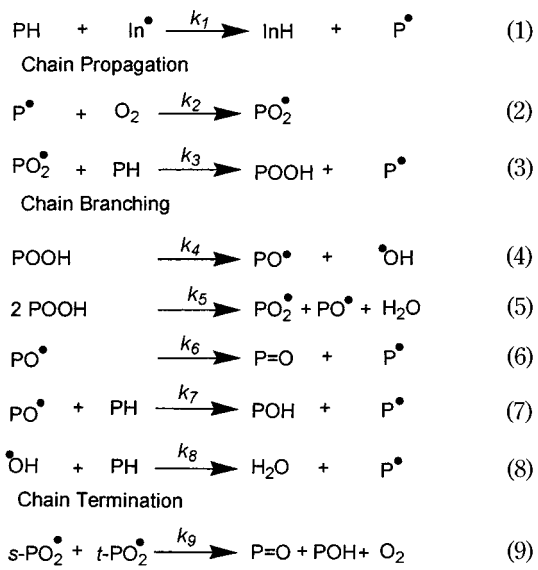

Hydroperoxide Decomposition CL Mechanism. Hydroperoxides are formed during the propagation step of auto-oxidation (eq 3, Scheme 1), when peroxy radicals abstract hydrogens from the polymer. Reich and Stivala[23] originally proposed decomposition of hydroperoxides as being responsible for CL during oxidation, although at the time this scheme was rejected by Vassil′ev[6] in favor of termination of peroxy radicals. In general, the unfavorable energetics[15] of this direct reaction process has led to limited acceptance of direct hydroperoxide decomposition being a source of CL. More recently, Achimsky et al.[25] have interpreted the linear dependency of the CL intensity (I_{CL}) on oxygen concentration as evidence for CL arising from the decomposition of hydroperoxides. Also Matisová-Rychlá et al.[24] have proposed that CL arises from the bimolecular

10.1021/ma001206n CCC: $20.00
Published on Web 02/15/2001

Scheme 2

Russell Mechanism for CL

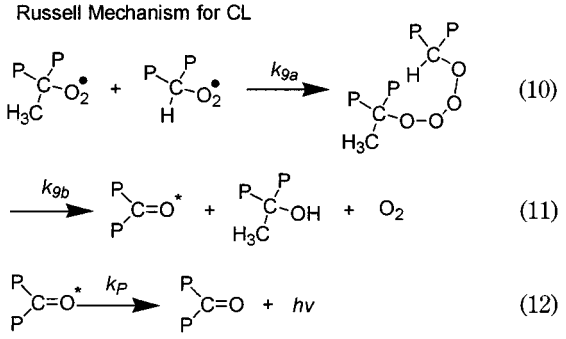

(10)

(11)

(12)

decomposition of hydroperoxides, although no precise reaction scheme was given.

Peroxy Radical Termination CL Mechanisms. The Russell mechanism[26] (shown in Scheme 2) accounts for termination of peroxy radicals, where at least one radical must have an α-hydrogen. This mechanism is currently the most accepted explanation for CL from auto-oxidizing systems. The primary reason for its popularity is that either a singlet oxygen or a triplet ketone molecule is required to be formed for the Wigner spin conservation rule to be obeyed. Singlet oxygen[21,27−29] and triplet carbonyls[9,20,30] have been detected in systems containing decomposing hydroperoxides and auto-oxidizing hydrocarbons or polymers. As well as complying with the Wigner spin conservation rule, the Russell mechanism also explains other experimental results associated with the reaction of peroxy radicals. For instance, Russell[26] observed a deuterium isotope effect during the termination of peroxy radicals formed during auto-oxidation of aralkyl hydrocarbons, which is consistent with Scheme 2. Howard and Ingold[31] also observed a deuterium isotope effect for *n*-butylperoxy, *sec*-butylperoxy, and cyclohexylperoxy radicals. Finally, the tetroxide intermediate has been detected and/or isolated during the interaction of secondary[29] and tertiary[32,33] peroxy radicals. It should be emphasized that the deuterium isotope effect is evidence for the mechanism of peroxy radical termination and does not itself provide evidence for CL production occurring via this mechanism.

A common feature of the Russell and hydroperoxide decomposition mechanisms is that the hydroperoxide or one of the peroxy radicals is required to be primary or secondary. The main sites of oxidation in PP are tertiary hydrogens, attack of which leads to tertiary hydroperoxides and peroxy radicals. However, secondary peroxy radicals and hydroperoxides can be formed following β-scission of alkoxy radicals (eq 6). Evidence for β-scission forming secondary alkyl radicals is the detection of secondary hydroperoxides,[34] peracids,[35] aldehydes,[36] and carboxylic acids,[36] which are all products derived from primary or secondary peroxy radicals.

There is little doubt that both termination of peroxy radicals and decomposition of hydroperoxides occur during thermal oxidation of polymers. The point of contention is whether these reactions are responsible for a significant amount of CL. The assignment of termination of peroxy radicals or decomposition of hydroperoxides as the reactions responsible for generation of CL in auto-oxidizing polymers has only been inferred from a limited number of results. Therefore, it would be significant to provide further evidence that would confirm or refute these mechanisms.

Further evidence could be obtained by comparing I_{CL}−time profiles with data from a complementary technique for oxidation product analysis such as FTIR emission spectroscopy[37−39] (FTIES). FTIES is also an inherently sensitive technique that can probe oxidation in real time. It has been shown, provided the sample is thin in order to limit reabsorption of the emitted radiation, that it is possible to obtain quantitative oxidation product profiles as a function of oxidation time.[38] Typically, samples are no thicker than 10 μm and less than 1 mm^2 in area. For certain types of commercially produced PP this corresponds to a single flattened reactor particle weighing on the order of 0.3 mg. The small sample size causes problems when attempting to compare CL and FTIES results. The reason for this is that small samples such as individual reactor particles have been demonstrated to have inherently different stabilities.[40] These differences were proposed to be due to varying levels of residual polymerization catalyst or stabilizer. These differences make it difficult to compare data from different microsamples with any degree of confidence. Furthermore, oxidation reactions are extremely sensitive to experimental conditions, such as temperature, sample shape, dimensions of the sample cell, composition of the oxidizing gas, and the gas flow rate. Oxidations carried out in different instruments will have experimental conditions that vary slightly, which will have an effect on the oxidation profiles collected. One way to overcome these problems is to couple a CL apparatus to an FTIES so that the sample can be analyzed simultaneously.

The most useful portion of IR spectra for oxidation product analysis is the carbonyl peak situated at 1680−1780 cm^{-1}. It has been shown, by spectral deconvolution, that the band in this region arises from species including γ-lactones, aldehydes, ketones and carboxylic acids.[36] Determination of the area under this peak from the series of spectra allows generation of total carbonyl accumulation curves. Because carbonyls are a major oxidation product in polyolefin thermal oxidation it would be interesting to correlate these profiles with CL data collected from the same sample at the same time. This paper discusses the results obtained from a CL-IES instrument for the thermal oxidation of PP.

Experimental Section

Materials. Unstabilized PP powder, Hostalen PPK0160 (Hoechst AG), melt flow index (MFI) at 230 °C/2.16 kg of 0.9 g/min, crystallinity by XRD of 45%, and Polychim A10TB, crystallinity by XRD of 31%, were used.[41] The Hostalen sample was Soxhlet extracted with AR hexane for 6 h. Individual reactor particles of PP were used for analysis. For FTIR emission spectroscopy, samples are required to be thin (<10 μm) and have intimate contact with the platinum hot plate to avoid formation of temperature gradients within the sample and absorption of the emitted light by the sample. Therefore, individual particles of PP were pressed between polished steel disks in an hydraulic press (under 10 tons for 20 min).

Monitoring of Thermal Polymer Oxidation with CL-IES. The flattened PP particles were analyzed with a CL apparatus coupled to a FT infrared emission spectrometer. The CL apparatus[40,42] and the FTIES[37] have been described previously. The emission cell in the FTIES was coupled to the CL apparatus via a multimode fiber optic probe (as shown in Figure 1). To prevent radiation from the HeNe timing laser in the FTIR emission spectrometer reaching the CL apparatus, electronic shutters were installed in front of, the photomultiplier tube in the CL apparatus and the window to the spectrometer. Analysis of the oxidizing sample was alternated

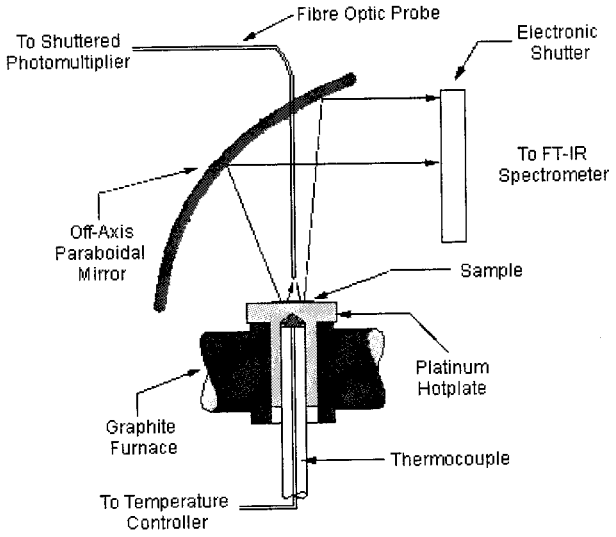

Figure 1. Schematic diagram of the emission cell of the CL-IES detailing the light path to the IR and CL detectors.

between CL apparatus and FTIES by sending TTL pulses to the shutters via a parallel port and a customized integrated circuit produced in-house. Automation of the analysis was controlled with in-house modified BioRad software and a CL data collection program written in-house.

FTIR emission spectra were averaged over 32 scans with a 4 cm^{-1} resolution (~25 s), and then the CL apparatus accumulated photon counts over a 35 s period. This sequence was repeated each minute during the oxidation of the polymer. CL data and FTIR data could therefore be obtained from an oxidizing single particle of PP almost simultaneously and in real time. For the runs where I_{CL} was of especially low intensity, the photon counts were averaged over longer time periods post analysis.

To convert the raw data from the FTIES to an emissivity spectrum, which is equivalent to an absorbance spectrum, a platinum background spectrum was subtracted and the result ratioed to a reference graphite spectrum.[37]

Oxidation of flattened PP particles in the CL-IES emission cell was performed at 150, 140, and 130 °C in an oxygen atmosphere, with a flow rate of 0.2 L min^{-1}.

Results and Discussion

Kinetic analysis of chemical data obtained by techniques such as CL and FTIES predict average concentrations of chemical species in a sample. For reactions in the gas phase or solutions of low viscosity, kinetic parameters and predicted concentrations are representative of the entire sample, because the assumption can be made that the system is homogeneous. However, for solutions with high viscosities and solids, such an assumption is not necessarily valid. The reason for this is that as viscosity increases the rates of bimolecular reactions tend to be dependent on diffusion rather than activation energy. For example, spatial patterns and reaction fronts have been observed for various auto-catalytic reactions occurring in unstirred solutions.[43,44] Consequently, for the oxidation of solid polymers the net effect is that oxidation is heterogeneous; i.e., oxidation is initially localized in submicroscopic domains[41,42,45,46] and then proceeds to spread to the remainder of the polymer during oxidation.

Kinetic analysis does not usually take into account heterogeneous oxidation because only average concentrations in a sample can be predicted. Therefore, any rate constant derived will have little fundamental significance. However, such kinetic analyses can still be useful for qualitatively studying the mechanism of reactions occurring in solids, e.g., analyzing the relationships between profiles of reactants, reactive intermediates, and products.

To understand how carbonyl and hydroperoxide profiles should relate to CL intensity (I_{CL}) profiles, kinetic analyses of the CL mechanisms need to be performed.

Kinetic Analysis of CL According To Mechanism. If we consider the Russell mechanism (Scheme 2) kinetically, eq 14 accounts for the generation of an excited carbonyl (P=O*) via interaction of two peroxy radicals and eq 13 accounts for nonradiative relaxation.

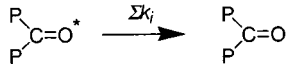

(13)

where ϕ_R is the fraction of oxidation products formed

$$\frac{d[P{=}O^*]}{dt} = k_9\phi_R[PO_2^\bullet]^2 - [P{=}O^*](k_P + \sum k_i) \quad (14)$$

in an excited electronic state during decomposition of the intermediate tetroxide in eq 11. Using the steady-state assumption that $(d[P{=}O^*])/dt = 0$, eq 14 becomes

$$[P{=}O^*] = \frac{k_9\phi_R[PO_2^\bullet]^2}{k_P + \sum k_i} \quad (15)$$

The rate of light emission, I_{CL} is given by

$$I_{CL} = k_P[P{=}O]^* = \phi_P\phi_R k_9[PO_2^\bullet]^2 \quad (16)$$

where $\phi_P = k_P/(k_P + \sum k_i)$ is the quantum yield of the light emission step in eq 12. For fixed experimental conditions $\phi_P\phi_R k_9$ is constant. Therefore, I_{CL} should be directly proportional to the square of the peroxy radical concentration.

$$I_{CL} \propto [PO_2^\bullet]^2 \quad (17)$$

If we treat the second literature mechanism for CL production, by decomposition of hydroperoxides, kinetically, eq 18 accounts for the generation of an electronically excited carbonyl.[23−25]

$$POOH \xrightarrow{k_d} P{=}O^* + H_2O \quad (18)$$

$$\frac{d[P{=}O^*]}{dt} = k_d\phi_R[POOH] - [P{=}O^*](k_P + \sum k_i) \quad (19)$$

Using the same logic as in eqs 14 and 15, the rate of light emission will be represented by eq 20.

$$I_{CL} = \phi_P\phi_R k_d[POOH] \quad (20)$$

For fixed temperature and experimental conditions, $\phi_P\phi_R k_d$ is constant. Therefore, I_{CL} should be directly proportional to the hydroperoxide concentration (eq 21).

$$I_{CL} \propto [POOH] \quad (21)$$

If, in the stationary state, the rate of initiation is controlled by decomposition of hydroperoxides[24] and the rate of termination is controlled by bimolecular recombination of peroxy radicals, then

$$k_d[\mathrm{POOH}] = k_9[\mathrm{PO}_2^\bullet]^2 \quad (22)$$

Therefore, the expressions for CL arising from peroxy radical termination (eq 16) and unimolecular hydroperoxide decomposition (eq 20) are kinetically equivalent. Hence, eq 21 should hold for chemiluminescence arising from either peroxy radical termination or unimolecular decomposition of hydroperoxides.

If CL arises through bimolecular decomposition of hydroperoxides[24] (eq 23), then eq 24 should describe the rate of light emission.

$$2\mathrm{POOH} \xrightarrow{k_{db}} \mathrm{P{=}O^*} + \mathrm{POH} + \mathrm{H_2O} \quad (23)$$

$$I_{CL} = \phi_P \phi_R k_{db}[\mathrm{POOH}]^2 \quad (24)$$

Hence, regardless of the mechanism in operation, I_{CL} will be proportional to some function of the hydroperoxide concentration. Therefore, the general relationship in eq 25 should describe the rate of light emission during PP oxidation, where γ is 1 or 2 depending on the CL mechanism.

$$I_{CL} \propto [\mathrm{POOH}]^\gamma \quad (25)$$

Kinetics of Oxidation from Emission Spectra. The primary route to formation of carbonyls is via decomposition of hydroperoxides. For example, unimolecular scission of hydroperoxides leads to formation of an alkoxy radical and a hydroxyl radical (eq 4). The alkoxy radical readily undergoes β-scission leading to formation of a variety of carbonyl groups (eq 6), which are observed via infrared emission spectroscopy.

Applying the stationary state approximation to the alkoxy radical

$$\frac{\mathrm{d}[\mathrm{PO}^\bullet]}{\mathrm{d}t} = k_4[\mathrm{POOH}] - [\mathrm{PO}^\bullet](k_6 + \sum k_i') = 0 \quad (26)$$

where $\sum k_i'$ may include pseudo-first-order processes such as hydrogen abstraction to give an alcohol.

If the principal route for the formation of alkoxy radicals is hydroperoxide decomposition, then their concentration is given by eq 27.

$$[\mathrm{PO}^\bullet] = \frac{k_4[\mathrm{POOH}]}{k_6 + \sum k_i'} \quad (27)$$

If β-scission is the dominant route for oxidation product formation then the rate of change of the carbonyl concentration becomes

$$\frac{\mathrm{d}[\mathrm{P{=}O}]}{\mathrm{d}t} = k_6[\mathrm{PO}^\bullet] = \phi_\beta k_4[\mathrm{POOH}] \quad (28)$$

where ϕ_β is the fraction of the alkoxy radicals, which undergo scission to produce carbonyls. Integration of (28) gives a relationship where the concentration of carbonyls at a given point in time is proportional to the integral of the hydroperoxide concentration (eq 29).

$$[\mathrm{P{=}O}]_t = \phi_\beta k_4 \int_0^t [\mathrm{POOH}]\, \mathrm{d}t \quad (29)$$

The relationship in eq 29 is consistent with results from the thermal and photooxidation of polyolefins and high impact polystyrene (HIPS). Scott[47,48] has shown that during the thermal and photooxidation of HIPS the hydroperoxide concentration rises to a maximum at the inflection of the carbonyl profile and then decays. During thermal oxidation of isotactic and atactic PP, Iring et al.[49] observed that the hydroperoxide profile rose rapidly to a maximum and decays while the carbonyl curve increases. Analyses of results indicate that, within error, the hydroperoxide oxidation time profile is equivalent to the derivative of the carbonyl profile.

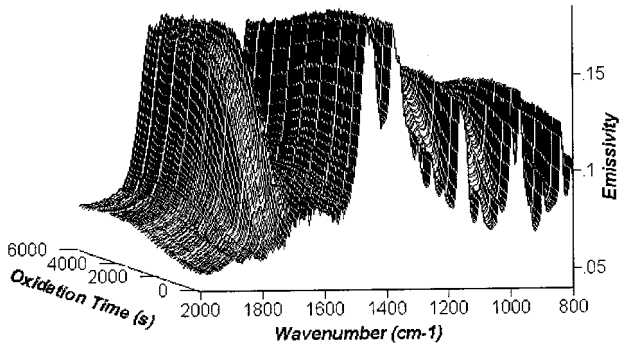

Figure 2. Time-resolved infrared emission spectra of PP oxidizing at 150 °C under an oxygen atmosphere.

When the value for [POOH] is substituted into eq 29 from eq 20 the relationship between the carbonyl concentration and the integral of the I_{CL}−time profile is obtained in eq 30

$$[\mathrm{P{=}O}]_t = \frac{\phi_\beta}{\phi_P \phi_R} \int_0^t I_{CL}\, \mathrm{d}t \quad (30)$$

If the initiation route is the bimolecular decomposition of hydroperoxides, then the same relation is obtained. Therefore, regardless of the CL mechanism (peroxy termination or hydroperoxide decomposition) the carbonyl growth curve should be proportional to the integral of the I_{CL}−time profile.

Comparison of I_{CL}−Time and Oxidation Product Profiles. The formation of carbonyls can be readily monitored with FTIES.[37−39] Figure 2 shows a typical set of time-resolved infrared emission spectra (600−2000 cm^{-1}) collected during a thermal oxidation of PP at 150 °C. The broad band that increases with time at 1680−1800 cm^{-1} consists of many overlapping bands due to various carbonyl species. These species include; α,β-unsaturated ketones (1690 cm^{-1}), carboxylic acids (1710 cm^{-1}), methyl ketones (1720 cm^{-1}), aldehydes (1725 cm^{-1}), esters (1745 cm^{-1}), and lactones (1780 cm^{-1}).[36] Essentially the increase in the area of the carbonyl band represents the cumulative amount of oxidation the system has undergone.

Changes in the broad peak at ~3500 cm^{-1}, which is due to the O−H stretch, [50] can be observed during oxidation. Unfortunately, contributions from this band result from the presence of carboxylic acids, [51] alcohols[52] and hydroperoxides[51] and so cannot be used as a quantitative measure of any of these species. Furthermore, the low sensitivity of infrared emission spectroscopy in the 2500−4000 cm^{-1} at 150 °C results in poor reproducibility.

Other peaks of interest are due to C−H vibrations of the polymer, which have been previously assigned by other authors from Raman and infrared spectroscopy.[53,54] The intensities of peaks due to bending modes decrease, but are less diagnostic due to interference from

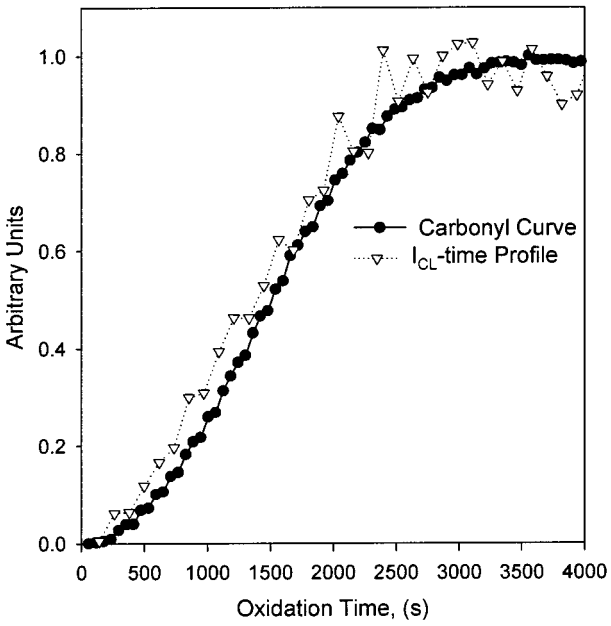

Figure 3. Comparison of the normalized I_{CL}−time profile (rate of light emission), with accumulation of carbonyl species during oxidation of PP (PPK0160) at 150 °C under an oxygen atmosphere.

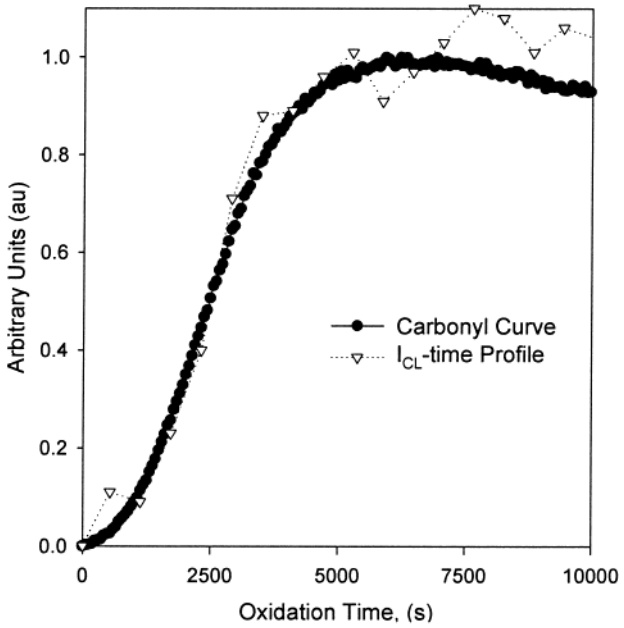

Figure 4. Comparison of the normalized I_{CL}−time profile (rate of light emission) and accumulation of carbonyl species during oxidation of PP (PPK0160) at 140 °C under an oxygen atmosphere.

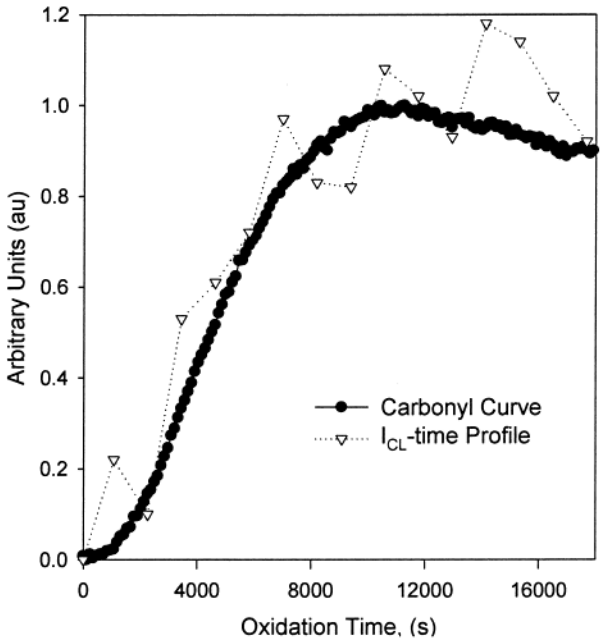

Figure 5. Comparison of the normalized I_{CL}−time profile (rate of light emission) and accumulation of carbonyl species during oxidation of PP (PPK0160) at 130 °C under an oxygen atmosphere.

a broad underlying band centered at 1200 cm^{-1}. This band is due to the C−O stretch of oxidation products such as alcohols, esters and ethers.[50]

As described earlier, by coupling a CL apparatus with a FTIES, carbonyl concentration−time and I_{CL}−time profiles can be measured simultaneously. Therefore, variations in band intensities with time due to different instrument reaction geometries, sample variability and uncertainties in the oxidation conditions can be removed. Oxidation of PP at 150 °C causes the carbonyl band area to increase to a maximum at 3000 s, and this then remains constant (Figure 3). The oxidation of PP results in an increase in the rate of light emission to a maximum also at 3000 s after the onset of oxidation, followed by a gradual decay (Figure 3). It is interesting to note that the I_{CL}−time profile is a good approximation of the carbonyl curve. This experiment was repeated for 13 other PPK0160 particles at 150 (data not shown), 140 (Figure 4), and 130 °C (Figure 5) and for A10TB particles (Figure 6). It should be noted that the collection efficiency of the fiber optic probe is at least 10 000 times less than the normal collection mode. Hence, observation of any signal at all from the instrument is a testament to the sensitivity of the CL apparatus.

The relationships derived in eqs 21 and 30 predicted that the I_{CL}−time profile would be proportional to the hydroperoxide concentration and that the integrated I_{CL}−time profile would be proportional to the carbonyl profile. Figure 7 shows that the integrated I_{CL}−time profile is not proportional to the carbonyl curve. Almost no CL is observed until carbonyl species are formed during the oxidation process. This demonstrates that the relationships derived from the "classical CL mechanisms", eqs 21 and 30, are incorrect and that I_{CL} is dependent on formation of carbonyl functional groups or some oxidation product that is generated at a similar rate as carbonyls. In fact, Figure 8 shows that the I_{CL}−time profile is proportional to the carbonyl curve (r^2 = 0.971). This demonstrates that the I_{CL}−time profile would not be proportional to the hydroperoxide concentration−time profile.

Explanations of CL-IES Results. There are at least two possible explanations of the CL-IES data. The first involves the formation an excited carbonyl via a classical mechanism; however, the triplet carbonyl participates in energy transfer with a more efficient phosphorescer, which accumulates in the polymer during oxidation. Therefore, as the concentration of this energy acceptor increases, I_{CL} increases accordingly. In fact, as early as 1965, Lundeen and Livingston proposed this type of mechanism for the oxidation of liquid hydrocarbons.[18] However, the effect on the interpretation of the I_{CL}−time profile was not discussed. Energy transfer mechanisms such as the one proposed have also been

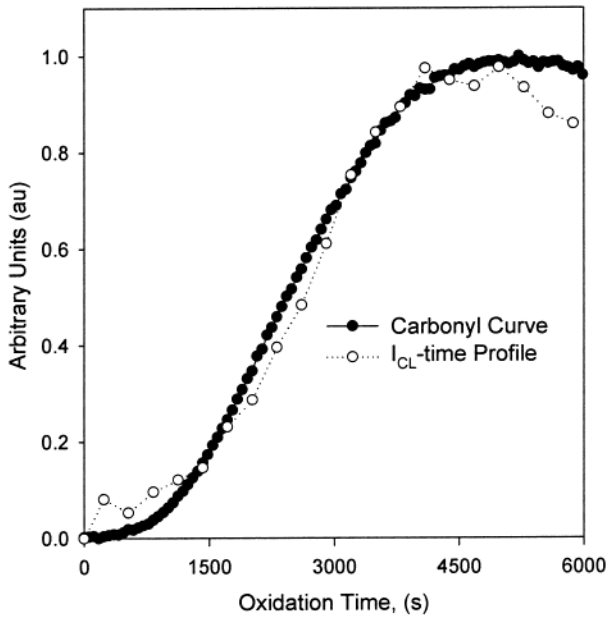

Figure 6. Comparison of the normalized I_{CL}−time profile (rate of light emission) to the accumulation of carbonyl species during oxidation of PP (A10TB) at 150 °C under an oxygen atmosphere.

Scheme 3

Energy Transfer Mechanism

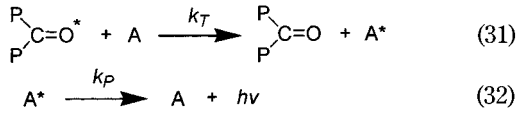

$$P_2C{=}O^* + A \xrightarrow{k_T} P_2C{=}O + A^* \quad (31)$$

$$A^* \xrightarrow{k_P} A + h\nu \quad (32)$$

reported to occur in other auto-oxidizing systems, such as during the auto-oxidation of tetrakis(dimethylamino)-ethylene (TDE).[55] The electronically excited state formed during the auto-oxidation of TDE is nonfluorescent, and CL is observed when energy transfer takes place between it and a TDE molecule, which is the emitting species. A possible mechanism is outlined in Scheme 3. If we treat this mechanism kinetically, where the excitation step is represented by eqs 11, 18, or 23 and the energy transfer step in Scheme 3, the rate of change of A* is given by

$$\frac{d[A^*]}{dt} = k_T[P{=}O^*][A] - [A^*](k'_P + \sum k''_i) = 0 \quad (33)$$

$$[A^*] = \frac{k_T[P{=}O^*][A]}{k'_P + \sum k''_i} \quad (34)$$

where $\sum k''_i$ represents radiationless rate coefficients for relaxation of A* to the ground state. In the presence of the energy acceptor, A, eq 14 can be transformed into eq 35 by inclusion of the energy transfer step:

$$\frac{d[P{=}O^*]}{dt} = k_9\phi_R[PO_2^\bullet] - [P{=}O^*](k_P + \sum k_i + k_T[A]) = 0 \quad (35)$$

$$[P{=}O^*] = \frac{k_9\phi_R[PO_2^\bullet]^2}{k_P + \sum k_i + k_T[A]} \quad (36)$$

Substituting into eq 34

$$[A^*] = \frac{k_T[A]k_9\phi_R[PO_2^\bullet]^2}{[k'_P + \sum k''_i](k_T[A] + k_P + \sum k_i)} \quad (37)$$

$$I_{CL} = k'_P[A^*] = \phi'_P\phi_{ET}(A)\phi_R k_9[PO_2^\bullet]^2 \quad (38)$$

where $\phi_{ET}(A)$ is the energy transfer efficiency, which is a function of the acceptor concentration. On the basis of the hydroperoxide decomposition mechanism for CL, the rate of light emission becomes

$$I_{CL} = k'_P[A^*] = \phi'_P\phi_{ET}(A)\phi_R k_d[POOH] \quad (39)$$

From this analysis it can be seen that I_{CL} will be dependent on both the concentration of the energy acceptor, A, and the hydroperoxide concentration. If the energy transfer process is highly efficient and exceeds the rate of both emission and radiationless decay of the excited carbonyl group, i.e. $k_T[A] \gg (k_P + \sum k_i)$ then the relationships for I_{CL} given in eqs 16 and 20 will apply except that ϕ_P is replaced by the luminescence quantum yield of the energy acceptor, A (ϕ'_P). As this is a bimolecular process, it will be expected to occur at high concentrations of A and then I_{CL} becomes independent of [A]. This is not observed in this system because I_{CL} is dependent on [A].

A second mechanistic scheme could involve the direct reaction of a carbonyl species (or other luminescent oxidation product) with high-energy reactive intermediates such as hydroperoxides, peroxides, peracids, peresters, or alkoxy radicals to yield CL in a single step. Organic peroxides are known to react with a range of electron donors including olefins, amines, and easily oxidizable hydrocarbons such as anthracene.[56] A path for the decomposition of *o*-xylylene peroxide involves electron transfer between a decomposition product of the peroxide, emitting light in the process.[57] The light emission was dependent on the concentration of the degradation product, similar to the dependence of PP I_{CL}−time profiles on carbonyl concentration, and was found to proceed via a chemically initiated electron exchange luminescence (CIEEL)[58] mechanism. Several other peroxides[59−66] have also been shown to react with easily oxidizable compounds (activators), such as 9,10-diphenylanthracene, rubrene, and perylene, via a CIEEL mechanism. CIEEL involves electron exchange between CL activator and peroxide, which converts the activator to a radical cation and the peroxide to a radical anion. The next step involves rearrangement of the radical anion, followed by charge recombination to form an excited activator, which relaxes to the ground state via emission of a photon. The quantum yields of CIEEL reactions vary greatly depending on the system. For example, peroxyoxalate systems, which are believed to involve an intermolecular CIEEL mechanism, have been demonstrated to have quantum yields of up to 0.3 E mol^{-1}.[67] However, other systems such as the decomposition of diphenoyl peroxide have been shown to have quantum yields on the order of 2×10^{-5} E mol^{-1}.[68] Nonetheless, these values are several orders of magnitude higher than those estimated for CL from the reaction of a pair of peroxy radicals ($\sim 10^{-8}$−10^{-10}).[20]

In a series of papers Lánská et al.[69−71] concluded that a source of CL during the auto-oxidation of polyamides and model polyamides was the redox reaction of a hydroperoxide and an aldehyde formed because of auto-oxidation. Although this example was not reported to

Scheme 4

Activated Chemiluminescence Mechanism

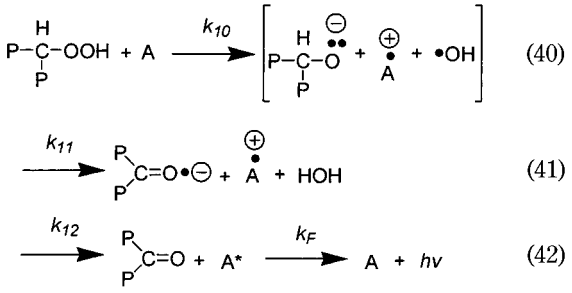

(40)

(41)

(42)

proceed via a CIEEL mechanism, the results reported are consistent with such a scheme.

From the literature evidence above, it can be proposed that chemically induced electron exchange luminescence occurs via a reaction between a peroxidic species (POOH) and some luminescent oxidation product (A) during thermal oxidation of PP (Scheme 4). This scheme will be an auto-catalytic relation since the catalyst is increasing throughout the reaction.

Treating such a scheme kinetically, where *A* is a fluorescent carbonyl produced during the oxidation of PP the overall reaction can be represented by eq 43, and the rate of change of A* is given by eq 44

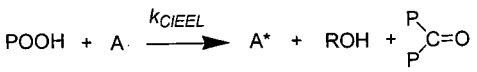

(43)

$$\frac{d[A^*]}{dt} = k_{CIEEL}[POOH][A] - [A^*](k'_p + \sum k''_i) = 0 \quad (44)$$

$$[A^*] = \frac{k_{CIEEL}[POOH][A]}{k'_p + \sum k''_i} \quad (45)$$

$$I_{CL} = k'_p[A^*] = \phi'_p k_{CIEEL}[POOH][A] \quad (46)$$

Similar to the energy transfer mechanism, eq 46 indicates that the I_{CL} for a CIEEL mechanism will be dependent on both the peroxide and oxidation product (activator) concentration. However, the results presented above indicate that I_{CL} is proportional to the carbonyl concentration; i.e., it is only dependent on the carbonyl concentration. A possible explanation for this discrepancy is that acyl peroxides, i.e. peracids or peresters, are participating in Scheme 3 or Scheme 4 to yield the majority of CL. Acyl peroxides will have significantly different kinetic profiles to alkyl hydroperoxides. The reason for the difference is that acyl peroxides are formed via oxidation of aldehydes. Therefore, the acyl peroxide concentration will be dependent on the aldehyde concentration, which will be proportional to the total carbonyl concentration.

A method to differentiate the energy transfer and CIEEL mechanisms would be to dope the polymer with energy acceptors. As discussed before, when [A] is large and an energy transfer mechanism is occurring then the I_{CL}−time profile should be proportional to the hydroperoxide concentration in eq 20.

Similarly, if the polymer is doped with a readily oxidizable compound that reacts with peroxides to yield CL without affecting the stability of the polymer, then the I_{CL}−time profile should be proportional to the hydroperoxide concentration (eq 46), because the concentration of A remains constant. Separation of these two mechanisms will require oxidation measurements of PP doped with energy transfer agents and CL activators with known electronic energy levels and redox potentials.

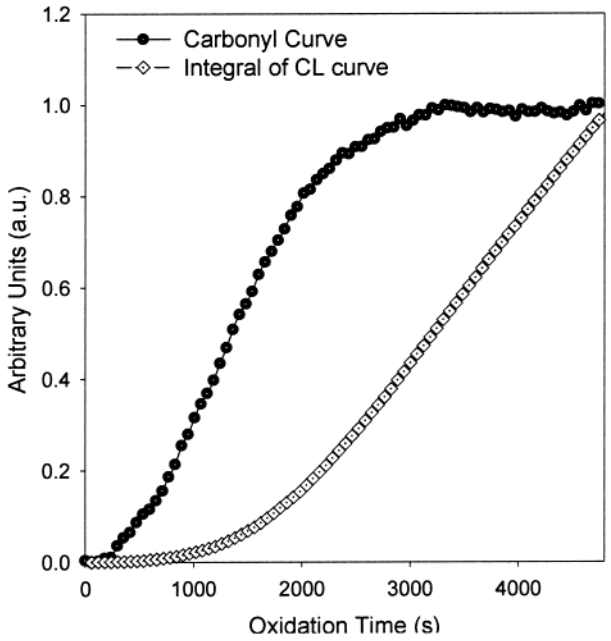

Figure 7. Comparison of accumulation of carbonyl species with the integral of I_{CL}−time profile. Data are for PP being oxidized at 150 °C under an oxygen atmosphere.

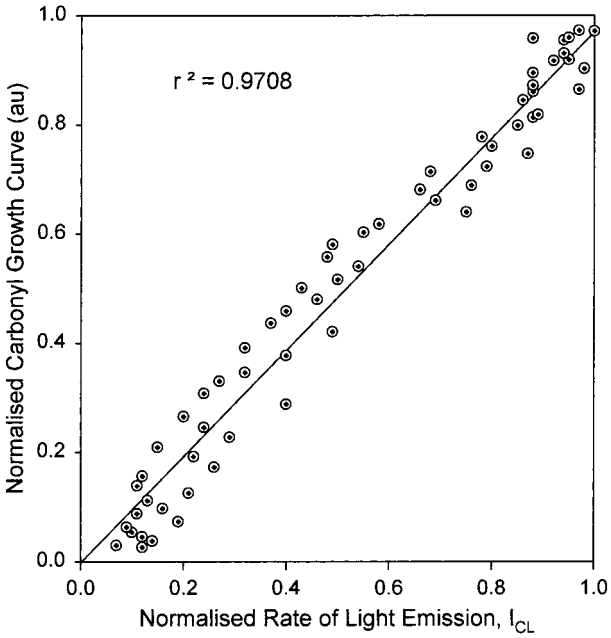

Figure 8. Correlation of I_{CL}−time profile (rate of light emission) and the accumulation of carbonyl species up to the maximum of both curves. $r^2 = 0.971$.

Conclusions

A CL apparatus was successfully coupled to a FTIR emission spectrometer, which allowed simultaneous analysis of PP thermal oxidation in real time. This allowed comparison of I_{CL}−time profiles with carbonyl concentration−time profiles. Kinetic analysis of "classical mechanisms" showed that the integral of the I_{CL}−

time profile should be proportional to the carbonyl curve. However, the carbonyl profile was not proportional to the integrated I_{CL}−time profile, which contradicts predictions from the kinetic analysis of peroxy radical termination or hydroperoxide decomposition. I_{CL} was found to be dependent on the rate of formation of a carbonyl species for the thermal oxidation of isotactic polypropylene between 130 and 150 °C. This result is significant for the interpretation of CL data for PP as it demonstrates that PP I_{CL}−time profiles are essentially proportional to the accumulation of carbonyls formed during oxidation.

The two possible mechanisms that were discussed are energy transfer from an excited carbonyl formed via a classical mechanism and the reaction of a carbonyl species with a peroxidic compound, which is likely to be an acyl peroxide. Further experimentation is required to determine which of these new mechanisms is correct or whether some other reaction is responsible.

Acknowledgment. The financial support of the Australian Research Council (Grant A29803983) and the support of the CIDC is greatly appreciated.

References and Notes

(1) Ashby, G. E. *J. Polym. Sci.* **1961**, *L*, 99−106.
(2) Shard, M. P.; Russell, C. A. *J. Appl. Polym. Sci.* **1964**, *8*, 983−995.
(3) Shard, M. P.; Russell, C. A. *J. Appl. Polym. Sci.* **1964**, *8*, 997−1006.
(4) Beutel, J. *J. Am. Chem. Soc.* **1971**, *93*, 2615−2621.
(5) Vassil'ev, R. F. *Nature* **1962**, *194*, 1276−1277.
(6) Vassil'ev, R. F. *Makromol. Chem.* **1969**, *126*, 231−238.
(7) Vassil'ev, R. F. *Makromol. Chem.* **1969**, *126*, 231.
(8) George, G. A. In *Developments in Polymer Degrdation-3*; Grassie, N., Ed.; Applied Science Publishers: London, 1981.
(9) Lacey, D. J.; Dudler, V. *Polym. Deg. Stab.* **1996**, *51*, 109−113.
(10) Tiemblo, P.; Gomez-Elvira, J. M.; Teyssedre, G.; Massines, F.; Laurent, C. *Polym. Deg. Stab.* **1999**, *65*, 113−122.
(11) Osawa, Z.; Wu, S.; Konoma, F. *Polym. Deg. Stab.* **1988**, *22*, 97−107.
(12) Phillips, D.; Anisimov, V.; Karpukhin, O.; Shiliapintokh *Nature* **1967**, *215*, 1163−1165.
(13) Höfert, M. *Photochem. Photobiol.* **1969**, *9*, 427−432.
(14) Vassil'ev, R. F. *Nature* **1962**, *196*, 668−669.
(15) Billingham, N. C.; Then, E. T. H.; Gijsman, P. *Polym. Deg. Stab.* **1991**, *34*, 263−277.
(16) Kron, A.; Stenberg, B.; Reitberger, T.; Billingham, N. C. *Polym. Deg. Stab.* **1996**, *53*, 119−127.
(17) Chien, J. C. W.; Boss, C. R. *J. Polym. Sci. A-1* **1967**, *5*, 3091.
(18) Lundeen, G.; Livingston, R. *Photochem. Photobiol.* **1965**, *4*, 1085−1096.
(19) Vassil'ev, R. F. *Prog. React. Kinet.* **1967**, *4*, 305−353.
(20) Kellogg, R. E. *J. Am. Chem. Soc.* **1969**, *91*, 5433−5466.
(21) Lee, S.-H.; Mendenhall, G. D. *J. Am. Chem. Soc.* **1988**, *91*, 4318−4323.
(22) Reich, L.; Stivala, S. S. *Rev. Macromol. Chem.* **1966**, *1*, 249−327.
(23) Reich, L.; Stivala, S. S. *Makromol. Chem.* **1967**, *105*, 74−82.
(24) Matisová-Rychlá, L.; Rychlý, J. *Polym. Deg. Stab.* **2000**, *67*, 515−534.
(25) Achimsky, L.; Audouin, L.; Verdu, J.; Rychla, L.; Rychly, J. *Eur. Polym. J.* **1999**, *35*, 557−563.
(26) Russell, G. A. *J. Am. Chem. Soc.* **1957**, *79*, 3871.
(27) Howard, J. A.; Ingold, K. U. *J. Am. Chem. Soc.* **1968**, *110*, 1056.
(28) Nakano, M.; Takayama, K.; Shimizu, Y.; Tsuji, Y.; Inaba, H.; Migita, T. *J. Am. Chem. Soc.* **1976**, *98*, 1974−1975.
(29) Bogan, D. J.; Celii, F.; Sheinson, R. S.; Coveleskie, R. A. *J. Am. Chem. Soc.* **1984**, *25*, 409−417.
(30) Lloyd, R. A. *Trans. Faraday Soc.* **1965**, *61*, 2182−2193.
(31) Howard, J. A.; Ingold, K. U. *J. Am. Chem. Soc.* **1968**, *90*, 1058.
(32) Mill, T.; Stringham, R. S. *J. Am. Chem. Soc.* **1968**, *90*, 1062−1064.
(33) Bartlett, P. D.; Guaraldi, G. J. *J. Am. Chem. Soc.* **1967**, *89*, 4799−4801.
(34) Valliant, D.; Lacoste, J.; Dauphin, G. *Polym. Deg. Stab.* **1994**, *45*, 1994.
(35) Gijsman, P.; Kroon, M.; Vanoorschot, M. *Polym. Deg. Stab.* **1996**, *51*, 3−13.
(36) Adams, J. H. *J. Polym. Sci. A* **1970**, *8*, 1077−1090.
(37) George, G. A.; Celina, M.; Vassallo, A. M.; Cole-Clarke, P. A. *Polym. Deg. Stab.* **1995**, *48*, 199−210.
(38) George, G. A.; Vassallo, A. M.; Cole-Clarke, P. A.; Celina, M. *Angew. Makromol. Chem.* **1995**, *232*, 105−118.
(39) Celina, M.; Ottesen, D. K.; Gillen, K. T.; Clough, R. L. *Polym. Deg. Stab.* **1997**, *58*, 15−31.
(40) Celina, M.; George, G. A.; Billingham, N. C. *Polym. Deg. Stab.* **1993**, *42*, 335−344.
(41) George, G. A.; Celina, M.; Lerf, C.; Cash, G.; Weddell, D. *Macromol. Symp.* **1997**, *115*, 69−92.
(42) Celina, M.; George, G. A. *Polym. Deg. Stab.* **1995**, *50*, 89−99.
(43) Johnson, B. R.; Scott, S. K.; Taylor, A. F. *J. Chem. Soc., Faraday Trans. 1* **1997**, *93*, 3733−3736.
(44) Chinake, C. R.; Simoyi, R. H. *J. Chem. Soc., Faraday Trans.* **1997**, *93*, 1345−1350.
(45) Livanova, N. M. *Polym. Sci. Ser. A* **1994**, *36*, 32.
(46) Blakey, I.; George, G. A. *Polym. Deg. Stab.* **2000**, *70*, 269−275.
(47) Ghaffar, A.; Scott, A.; Scott, G. *Eur. Polym. J.* **1976**, *12*, 615−620.
(48) Scott, G. In *Developments in Polymer Degradation − 1*; Applied Science Publishers: London, 1977.
(49) Iring, M.; László-Hedvig, Z.; Tüdös, F.; Kelen, T. *Polym. Deg. Stab.* **1983**, *5*, 467−480.
(50) Lin-Vien, D.; Colthup, N. B.; Fateley, W. G.; Grasselli, J. G. *The Handbook of Infrared and Raman Characteristic Frequencies of Organic Molecules*, 1st ed.; Academic Press: San Diego, CA, 1991.
(51) Gugumus, F. *Polym. Deg. Stab.* **1999**, *63*, 525−529.
(52) Carlsson, D. J.; Brousseau, R.; Zhang, C.; Wiles, D. M. *Polym. Deg. Stab.* **1987**, *17*, 303−318.
(53) Arruebarrena de Baez, M. A.; Hendra, P. J.; Judkins, M. *Spectrochim. Acta* **1995**, *51*, 2117.
(54) Snyder, R. G.; Schachtschneider, J. H. *Spectrochim. Acta* **1964**, *20*, 853−869.
(55) Winberg, H. E.; Downing, J. R.; Coffman, D. D. *J. Am. Chem. Soc.* **1965**, *87*, 2054−2055.
(56) Zupancic, J. J.; Horn, K. A.; Schuster, G. B. *J. Am. Chem. Soc.* **1980**, *102*, 5279−5285.
(57) Smith, J. P.; Schrock, A. K.; Schuster, G. B. *J. Am. Chem. Soc.* **1982**, *104*, 1041−1047.
(58) Schuster, G. B. *Acc. Chem. Res.* **1979**, *12*, 366−373.
(59) Koo, J.-y.; Schuster, G. B. *J. Am. Chem. Soc.* **1978**, *100*, 4496−4503.
(60) Dixon, B. G.; Schuster, G. B. *J. Am. Chem. Soc.* **1979**, *101*, 3116−3118.
(61) Adam, W.; Erden, I. *J. Am. Chem. Soc.* **1979**, *101*, 5692−5696.
(62) Van Gompel, J.; Schuster, G. B. *J. Org. Chem.* **1987**, *52*, 1465−1468.
(63) Sakanishi, K.; Nugroho, M. B.; Kato, Y.; Yamazaki, N. *Tetrahedron Lett.* **1994**, *35*, 3559−3562.
(64) Stevani, C. V.; Baader, W. J. *J. Phys. Org. Chem.* **1997**, *10*, 593−599.
(65) McCapra, F.; Leeson, P. D. *J. Chem. Soc., Chem. Commun.* **1979**, 114−117.
(66) Schmidt, S. P.; Schuster, G. B. *J. Am. Chem. Soc.* **1978**, *100*, 1966−1968.
(67) Catherall, C. L. R.; Palmer, T. F.; Cundall, R. B. *J. Biolumin. Chemilumin.* **1989**, *3*, 147−154.
(68) Catalani, L. H.; Wilson, T. *J. Am. Chem. Soc.* **1989**, *111*, 2633−2639.
(69) Lánská, B.; Matisová-Rychlá, L.; Rychly, J. *Polym. Deg. Stab.* **1998**, *61*, 119−127.
(70) Lánská, B.; Matisová-Rychlá, L.; Brozek, J.; Rychlý, J. *Polym. Deg. Stab.* **1999**, *66*, 433−444.
(71) Lánská, B.; Doskocilova, D.; Matisová-Rychlá, L.; Puffr, R.; Rychlý, J. *Polym. Deg. Stab.* **1999**, *63*, 469−480. *To whom correspondence should be directed. email g.george@qut.edu.au

MA001206N